Tetrahedron: *Asymmetry* 27 (2016) 130–135

Contents lists available at ScienceDirect

Tetrahedron: *Asymmetry*

journal homepage: www.elsevier.com/locate/tetasy

Reversal of enantioselectivity induced by the achiral part of an organocatalyst in a Diels–Alder reaction

Trupti S. Tawde, Swapnil J. Wagh, Jai V. Sapre, Vaibhav N. Khose, Purav M. Badani, Anil V. Karnik *

Department of Chemistry, University of Mumbai, Mumbai 400 098, India

ARTICLE INFO

Article history:
Received 16 December 2015
Accepted 4 January 2016
Available online 12 January 2016

ABSTRACT

A new series of chiral organocatalysts was developed by attaching achiral heterocyclic units via a methylene group to (*S*)-2-hydroxyethylbenzimidazole for the asymmetric Diels–Alder reaction between anthrone enolate and maleimides. While organocatalysts with pyridine, quinoline, and 1,3,4-oxadiazole achiral heterocyclic subunits gave Diels–Alder adducts with an (*S*,*S*)-configuration, the organocatalyst with a benzotriazole subunit caused formation of the (*R*,*R*)-configuration for the Diels–Alder adducts

1. Introduction

The Diels–Alder reaction is one of the most prominent C–C bond forming reactions. While Lewis acid catalyzed asymmetric Diels–Alder reactions have seen phenomenal growth in terms of efficiency and enantioselectivity;[1] reasonable levels of enantioselectivities[2] have also been observed in chiral base induced generation of diene components undergoing cycloadditions with dienophiles. Generation of the enolate of anthrone by use of a chiral base for asymmetric Diels–Alder reactions with maleimides is a representative example of this class of Diels–Alder reactions. Prominent contributions to this reaction have come from Kagan,[3] Yamamoto,[4] Wong,[2b] Gobel,[2c] and others.[2d–f]

Chiral organocatalysis induced asymmetric synthesis is a very delicate phenomenon. The stereochemical outcome is the result of difference in the geometries of the competing diastereomeric transition states. To have better control over the stereochemical outcome of these reactions, all the parameters contributing to the transition state must be fully understood. Typically asymmetric synthesis relies upon several parameters, which include the type of chiral influence, its proximity to the reaction site, availability of additional binding sites, etc. For example, many catalysts have exhibited marked improvement in enantioselectivity simply by attachment of an achiral unit such as a thiourea.[5]

A literature search reveals that in the recent years, chiral molecules with two heterocyclic rings[6] have become functional alternatives to thioureas[5] and guanidine[7] based organocatalysts, due to formation of distinctly different rigid diastereomeric transition states via hydrogen bond interactions and enhanced basic nature. In the past few years this structural motif has been successfully explored for the development of organocatalysts for a variety of asymmetric transformations such as Michael reactions,[8] Aldol reactions,[9] Diels–Alder reactions[10] and in kinetic resolutions.[11] Due to the significant role that these chiral heterocycle tweezers can play in numerous applications, the asymmetric synthesis of enantiopure heterocycles using chiral heterocyclic tweezers continues to be a highly active field of research.

2. Results and discussion

Recently we reported[2a] the use of (*S*)-2-hydroxyethylbenzimidazole [HEB **1**] for the Diels–Alder reaction between the enolate from anthrone **3** and maleimides **4** with low to moderate enantioselectivity. Obviously the chiral catalyst employed was not providing sufficiently effective diastereomeric transition states to afford satisfactory levels of enantioselection.

Then having realized that HEB **1** is not an optimum catalyst for the reaction between anthrone enolate **3** and maleimide **4**,[2a] we decided to structurally modify the HEB **1** by attaching a nitrogen containing heteroaryl ring to the HEB **1** by a flexible arm. It has been expected that the conjugate acid of the heteroaryl moiety, after abstracting the proton from the anthrone, would remain in the close-proximity to the benzimidazole ring and the hydroxyl group would then have hydrogen bonding interaction with the maleimide part resulting in good levels of enantioselection. Based on this premise, chiral tweezers **2a–d** (Fig. 1) were developed by a simple synthetic protocol shown in Scheme 1.

All the tweezers, namely, (*S*)-(−)-*N*-(methyl-2′-pyridyl)-2-(α-hydroxyethyl)benzimidazole [Pyr-HEB] **2a**, (*S*)-(−)-*N*-(methyl-2′-quinolyl)-2-(α-hydroxyethyl)benzimidazole [Qn-HEB] **2b**,

* Corresponding author. Tel.: +91 022 26526091; fax: +91 022 26528547.
E-mail address: avkarnik@chem.mu.ac.in (A.V. Karnik).

http://dx.doi.org/10.1016/j.tetasy.2016.01.002
0957-4166/

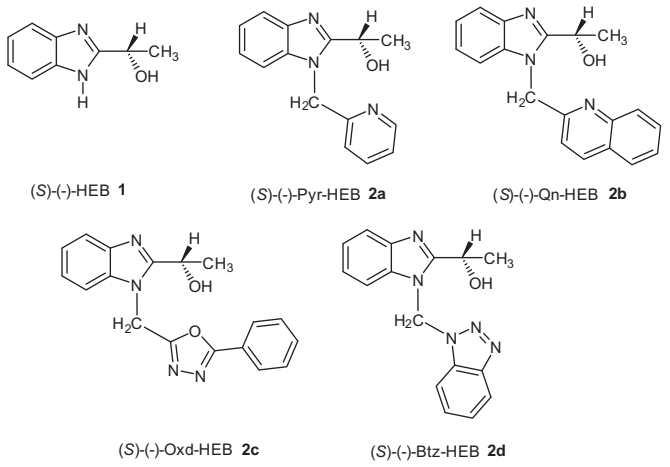

Figure 1. Proposed chiral tweezers **1**, **2a–d**.

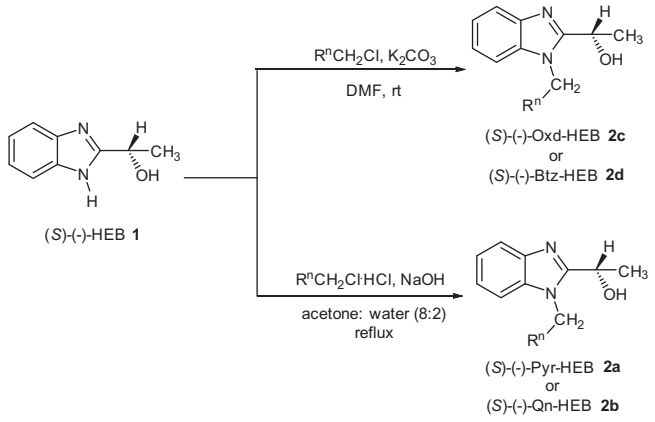

Scheme 1. Synthetic pathway for preparation of chiral base tweezers **2a–d**.

(*S*)-(−)-*N*-[methyl-2′-5′(phenyl-1′,3′,4′-oxadiazolyl)]-2-(α-hydroxyethyl) benzimidazole [Oxd-HEB **2c**], (*S*)-(−)-*N*-(methyl-1′-benzotriazolyl)-2-(α hydroxyethyl)benzimidazole [Btz-HEB **2d**] were obtained in good yields and with excellent enantiopurities. A notable feature of ^{1}H NMR spectra of these compounds is the appearance of two doublets for the linker 'CH_2' group, which clearly indicated diastereotopic nature of the 'CH_2' protons in these compounds and interestingly indicated that these compounds exhibit some levels of conformational preferences even in free form.

When we carried out the initial experiments of the Diels–Alder reaction between anthrone enolate **3**, generated by chiral tweezers **2a–d** and maleimide **4a–g**, mixed results were obtained; all the tweezers were not found to be uniformly efficient and tweezers **2a–c** gave the major stereoisomer of the Diels–Alder adduct **5a–g** as (*S*,*S*), while the tweezer **2d** gave (*R*,*R*) as the major stereoisomer of **5a–g** (Scheme 2).

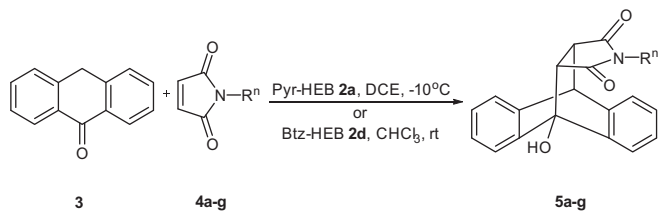

Scheme 2. Substrate scopes of anthrone **3** and maleimide **4** for asymmetric Diels–Alder reaction.

This serendipitous finding was then further investigated. All the chiral tweezers employed by us have been developed from a common synthon, (*S*)-2-hydroxyethylbenzimidazole [HEB **1**], naturally, **2a–2d**, have the same stereogenic center with the same configuration, that is (*S*). We were anticipating enhanced enantioselectivities with **2a–2d**, in relation to **1**,[2a] due to the additional nitrogen containing heterocycle, however we unexpectedly stumbled upon reversal of enantioselectivity for the Diels–Alder adduct **5a–g** when **2d** was used as the chiral organocatalyst. The answer to this puzzling observation apparently lies in the nature of interactions between the protonated heteroaryl rings and benzimidazole moiety, which are proposed to be different for transition states involving **2a–2c** and **2d**.

Unusual reversal of enantioselectivity has been reported by many groups in a variety of reactions,[12] for reactions employing chiral metal-based catalysts,[13] and with a few organocatalysts.[14] The chiral chemists would expect to see the opposite effect of the chiral metal-based catalysts/chiral organocatalysts with opposite configuration affording mirror image enantioselectivity, as in the case of Sharpless epoxidation.[15] However, there are examples where the chiral influence was the same and the difference in achiral reaction parameters such as pressure,[16] temperature,[17] solvent,[18] achiral additives, and[19] type of Lewis acids[20] employed have influenced the reversal of enantioselectivity. Interesting examples have also been found where the absolute configuration in the chiral catalyst is the same and only a slight difference in the catalyst structure resulted in complete opposite enantiofacial selectivity.[21]

While organocatalytic asymmetric Diels–Alder reaction between the enolate of anthrone **3** and maleimide **4** has been reported[2–4] by many groups, to the best of our knowledge, reversal of enantioselectivity while employing catalysts with same absolute configuration has not been reported previously for this reaction.

The mechanism proposed by Yamammoto[4a] and others[2b,3] to account for the stereochemical outcome in this reaction appears satisfactory. On these lines in our case we propose that, the acidic proton of the anthrone **3** was abstracted by the chiral catalysts **2a–d**, converting anthrone **3** into its enolate form with a protonated amine as its counterion. The chiral catalyst with a hydroxyl group present at the stereogenic center then formed an H-bond with the maleimide. Thus the chiral amine was partially bonded to the diene part and the dienophile part to induce stereoselectivity. In the case of approach of the maleimide **4** from the right hand side, an (*S*,*S*)-configuration was expected, on the other hand in the case of the approach of the maleimide **4** from the left hand side, a (*R*,*R*) configuration could be expected.

To account for the stereochemical outcome of the asymmetric Diels–Alder reaction using the chiral organocatalyst **1** to **2a–d**; various possibilities were considered. Possibility number one was obviously the protonation of the most basic benzimidazole nitrogen, the unsubstituted nitrogen in the benzimidazole ring, the conjugate acid thus formed, would remain close to the anion of anthrone and the hydroxyl group would then have a hydrogen bonding interaction with the maleimide part resulting in the 11 member cyclic transition state Figure 2A. In such a scenario all the catalysts **2a–2c** would have resulted in Diels–Alder adducts with the same configuration, for example, (*S*,*S*); as the additional heterocyclic ring arm would have been largely ineffective in influencing the stereochemical outcome of the reaction. Since a different configurational isomer of the Diels–Alder adduct was obtained in the case of **2d**, we had to look for some other possibility.

Possibility number two could be protonation of the nitrogen on the heteroaryl ring attached to the benzimidazole. The conjugate acid thus formed then would remain partially bonded to the oxygen anion of the anthrone enolate. Again the hydroxyl group of the benzimidazole ring could be expected to hydrogen bond with

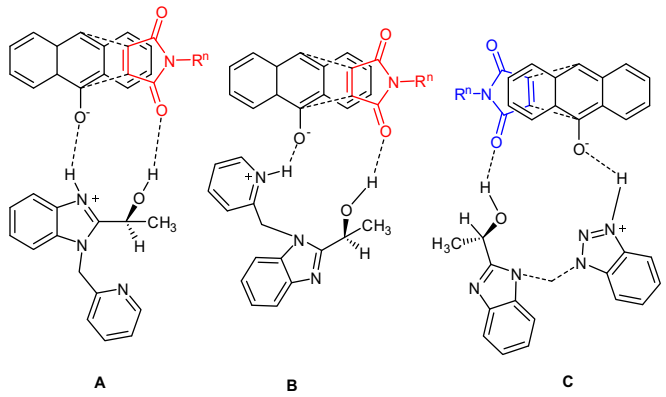

Figure 2. Transition state model of approach of maleimide **4** toward anthrone enolate with (A) catalyst Pyr-HEB **2a** involving protonated benzimidazole nitrogen, (B) catalyst Pyr-HEB **2a** involving protonated pyridine nitrogen (C) catalyst Btz-HEB **2d** involving protonated benzotriazole nitrogen.

the maleimide part. This could result in a large sized 14 or 15 membered transition state; this naturally would be less crowded than the medium sized 11 membered transition state. This is illustrated in Figure 2B and C.

Based on this possibility we propose that though the nitrogen atom on the benzimidazole ring was expected to be the site for protonation, the actual protonation could be taking place on the nitrogen atom of the heteroaryl nitrogen atom due to formation of larger, less crowded 14/15 membered transition state complex. This protonated base then would remain bonded to the enolate of anthrone **3**. The benzimidazole part could possibly have an attractive interaction with the protonated flexible arm heterocycle and would remain in the close proximity to the benzimidazole ring. The side arm of the benzimidazole ring with a stereogenic center and hydroxyl group would be partially bonded via a hydrogen bond with the maleimide part. This would make the approach of the maleimide facile from the right hand side, and the predominant stereoisomer obtained would be (*S*,*S*). This accounts for the stereochemical outcome as (*S*,*S*), when **2a**–**2c** were employed as the organocatalysts (Fig. 2B).

When benzotriazolyl side arm **2d** with three nitrogen atoms and a fused ring was employed, the benzotriazole ring after protonation at N-3, possibly could not remain in the same plane and in close proximity to the benzimidazole ring due to repulsion between nitrogen atoms on benzotriazole and nitrogen atoms on benzimidazole and also due to the bulk of the benzotriazole. The two benzo-fused azoles rings would be forced as far away as possible. This would make the approach of the maleimide **4** difficult from the right hand side, thus the maleimide part was forced to approach from the left hand side (Fig. 2C) and consequently the predominant stereoisomer would be (*R*,*R*).

While the best results, in terms of the extent of enantioselectivity, were obtained in case of tweezer Pyr-HEB **2a**. Tweezers Pyr-HEB **2a** and Btz-HEB **2d** were evaluated for the optimal conditions by investigating the effect of solvents and the effect of temperature. Lowering the temperature of the reaction using Pyr-HEB **2a** from room temperature to −10 °C, extended the reaction time yet furnished better enantioselectivities, up to 88% ee. On further lowering the temperature, the cycloaddition was retarded. While no reaction progress was observed for the reaction using Btz-HEB **2d** at lower temperature.

Under the optimized conditions, we explored the scope of the asymmetric Diels–Alder reaction and the results are summarized in Table 1. A notable feature being while tweezer **2a** gave better enantioselectivities for *N*-alkyl maleimides, tweezer **2d** was found to afford better enantioselectivity with *N*-phenyl maleimide. Table 1 presents the results under optimal conditions.

3. Conclusion

In conclusion, we have come across a serendipitous finding that a change in the achiral part of chiral organocatalysts caused reversal in enantioselectivity of the Diels–Alder adducts, even though the stereogenic center in these organocatalysts had the same configuration. The possible reason to this observation could be due to the repulsive interaction between the benzimidazole part and the protonated benzotriazole part in **2d**, unlike in other organocatalysts **2a**–**2c**, where attractive interactions appear to be dominant. These results can have useful applications in understanding the parameters responsible for enantioselectivities and contribute to the development of other organocatalysts.

4. Experimental

4.1. General

^{1}H NMR, ^{13}C NMR, COSY, DEPT-135, HSQC spectrums were recorded in $CDCl_3$ and DMSO-d_6 using spectrometer operating at 300 MHz (^{13}C NMR, DEPT-135 are recorded at 75 MHz) with TMS as an internal standard Multiplicities are indicated as s (singlet), d (doublet), t (triplet), q (quintet), and m (multiplet), and coupling constants (*J*) are reported in Hertz. Splitting patterns that could not be easily interpreted are designated as multiplet (m). IR spectra were recorded on FT-IR instrument. Enantiomeric excesses were determined by chiral HPLC analysis. The absolute configurations of the known products were assigned by chiral HPLC and specific rotation comparisons with the reported data.[2–4] Melting points

Table 1
Substrate[a] scope of anthrone **3** and maleimide **4a**–**g** for asymmetric Diels–Alder reactions

Entry	*N*-Substitute maleimide **4**, R^n=		Adduct **5**	With Pyr-HEB **2a**			With Btz-HEB **2d**		
				Yield[b] (%)	ee[c] (%)	Configuration[d]	Yield[b] (%)	ee[c] (%)	Configuration[d]
1	CH_3	**4a**	**5a**	94	63	(*S*,*S*)	85	12	(*R*,*R*)
2	C_2H_5	**4b**	**5b**	90	88	(*S*,*S*)	75	23	(*R*,*R*)
3	C_3H_7	**4c**	**5c**	90	14	(*S*,*S*)	88	22	(*R*,*R*)
4	*tert*-Bu	**4d**	**5d**	87	48	(*S*,*S*)	79	30	(*R*,*R*)
5	Bn	**4e**	**5e**	75	78	(*S*,*S*)	86	24	(*R*,*R*)
6	Ph	**4f**	**5f**	65	17	(*S*,*S*)	91	73	(*R*,*R*)
7	*p*-$CH_3OC_6H_4$	**4g**	**5g**	60	16	(*S*,*S*)	82	23	(*R*,*R*)

[a] All reactions were carried out using *N*-substituted maleimide **4** (0.5 mmol), anthrone **3** (0.5 mmol) in 5 ml of solvent with 10 mol % of catalyst **2a**/**2d** at the specified temperature.
[b] Isolated yield after column chromatography.
[c] The enantiomeric excess was determined by Chiral HPLC using Chiralcel AD column of Diacel.
[d] Configuration was determined by comparison of the specific rotation reported in the literature.[2–4]

were recorded and uncorrected. The progress of the reaction was monitored by thin-layer chromatography (TLC) using silica gel. All reagents and solvents were commercially available with analytical grade and used as received.

4.2. Synthesis and characterization of compounds 2a–d

4.2.1. Procedure A: preparation of chiral tweezer 2a and 2b

To the solution of sodium hydroxide (0.37 g, 9.25 mmol) in 10 ml of Acetone/water (8:2), (*S*)-(−)-2-(α-hydroxyethyl)benzimidazole (HEB) **1** (1 g, 6.17 mmol), 2-(chloromethyl)pyridine hydrochloride (1 g, 6.17 mmol)/2-(chloromethyl)quinoline hydrochloride (1.32 g, 6.17 mmol) were added. The reaction mixture was refluxed for 8 h. The reaction was monitored for complete consumption of HEB **1** by TLC. After completion of reaction acetone was removed by distillation. The remaining residue was diluted with water and stirred at room temperature. The solid obtained was filtered and dried.

4.2.2. Procedure B: preparation of chiral tweezer 2c and 2d

To the solution of (*S*)-(−)-2-(α-hydroxyethyl)-benzimidazole HEB **1** (1 g, 6.17 mmol) and K_2CO_3 (1.27 g, 9.25 mmol) in DMF (50 mL) 2-(chloromethyl)-5-phenyl-1,3,4-oxadiazole (1.20 g, 6.17 mmol)/ 1-(chloromethyl)-1*H*-benzotriazole (1.04 g, 6.17 mmol) was added. The reaction mixture was stirred at room temperature for 7 h. The reaction was monitored for complete consumption of HEB **1** by TLC. After completion of reaction mixture was poured into crushed ice. The solid obtained was filtered and dried.

4.2.2.1. (*S*)-(−)-*N*-(Methyl-2′-pyridyl)-2-(α-hydroxyethyl)benzimidazole Pyr-HEB 2a. Compound **2a** was prepared by procedure **A**; colorless solid, 1.55 g, 99% yield, melting point: 95 °C; $[\alpha]_D^{25} = -39$ (*c* 1, $CHCl_3$); IR (KBr, cm^{-1}): ν_{max} 3212, 2926, 1594, 1434, 1318, 732; ^{1}H NMR (300 MHz, $CDCl_3$): δ 8.42–8.41 (m, Ar-H, 1H), 7.74–7.58 (m, Ar-H, 2H), 7.26–7.14 (m, Ar-H, 5H), 6.33 (s, 1H, OH), 5.55 (two doublets, J = 16.2 Hz, J = 15.9 Hz, 2H), 5.30 (q, 1H), 1.79 (d, 3H, J = 6.6 Hz); ^{13}C NMR (75 MHz, $CDCl_3$): δ 156.58, 154.78, 149.48, 142.04, 137.65, 135.14, 123.25, 122.88, 122.37, 122.15, 120.00, 109.43, 62.57, 48.71, 21.41; DEPT-135 (75 MHz, $CDCl_3$): One negative peak at δ 48.71 for one 'CH_2' group; COSY (300 MHz, $CDCl_3$): Signal indicating coupling between 'H' of CH (δ 5.30) and 'H' of CH_3 (δ 1.79). Also signal at δ 5.50 ppm is correlated to the signal at δ 5.47 ppm, indicating coupling between protons of CH_2 group; ESI MS: m/z (M^+) value at 254.13; Anal. Calcd for $C_{15}H_{15}N_3O$: C, 71.13; H, 5.97; N, 16.59. Found: C, 71.02; H, 5.91; N, 16.52. Chiral HPLC: Chiralpak IB column of diacel, *i*-PrOH/Hexane 10:90, Flow rate 0.6 mL/min, λ_{max} = 254 nm, t_{major} = 83.73 min, t_{minor} = 75.53 min, 100% ee.

4.2.2.2. (*S*)-(−)-*N*-(Methyl-2′-quinolyl)-2-(α-hydroxyethyl)benzimidazole Qn-HEB 2b. Compound **2b** was prepared by procedure **A**; colorless solid, 1.81 g, 97% yield; melting point: 105 °C; $[\alpha]_D^{25} = -17$ (*c* 1, $CHCl_3$); IR (KBr, cm^{-1}): ν_{max} 3221, 2927, 2866, 1593, 1458, 1089, 735; ^{1}H NMR (300 MHz, $CDCl_3$): δ 8.22–7.24 (m, Ar-H, 10H and s, OH, 1H), 5.84 (two doublets, J = 15.9 Hz, J = 16.2 Hz, 2H), 5.48 (q, 1H), 1.88 (d, 3H, J = 6.6 Hz); ^{13}C NMR (75 MHz, $CDCl_3$): δ 156.63, 155.19, 147.28, 142.10, 138.14, 135.26, 130.51, 128.46, 127.60, 127.47, 127.17, 122.98, 122.49, 120.10, 119.64, 109.41, 62.66, 49.24, 21.46; DEPT-135 (75 MHz, $CDCl_3$): One negative peak at δ 49.23 for one 'CH_2' group; COSY (300 MHz, $CDCl_3$): Signal indicating coupling between 'H' of CH (δ 5.48 ppm) and 'H' of CH_3 (δ 1.88 ppm). Also the signal at δ 5.78 ppm is correlated to the signal at δ 5.76 ppm, indicating coupling between protons of CH_2 group; ESI MS: m/z (M^+) value at 304.19; Anal. Calcd for $C_{19}H_{17}N_3O$: C, 75.23; H, 5.65; N, 13.85. Found: C, 75.14; H, 5.72, N, 13.91; Chiral HPLC: Chiralpak IB column of diacel, *i*-PrOH/Hexane 10:90, Flow rate 0.6 mL/min, λ_{max} = 254 nm, t_{major} = 12.61 min, t_{minor} = 17.32 min, 87% ee.

4.2.2.3. (*S*)-(−)-*N*-[Methyl-2′-5′(phenyl-1′,3′,4′-oxadiazolyl)]-2-(α-hydroxyethyl)benzimidazole Oxd-HEB 2c. Compound **2c** was prepared by procedure **B**; Colorless solid, 1.71 g, 97% yield; melting point: 145 °C; Specific rotation: $[\alpha]_D^{25} = -47$ (*c* 1, $CHCl_3$); IR (KBr, cm^{-1}): ν_{max} 3473, 3142, 2980, 1609, 1527, 1449, 1321, 1161, 1096, 767; ^{1}H NMR (300 MHz, DMSO-d_6): δ 7.93–7.90 (m, 2H), 7.67–7.52 (m, 5H), 7.31–7.20 (m, 2H), 6.04 (unresolved singlet, 2H), 5.82 (d, 1H, J = 6.2 Hz –OH), 5.16 (t, 1H, J = 6.6 Hz), 1.64 (d, 3H, J = 6.6 Hz); ^{13}C NMR (75 MHz, DMSO-d_6): δ 164.42, 162.40, 156.11, 141.52, 135.43, 131.94, 129.22, 126.39, 123.0, 122.60, 121.92, 119.12, 110.09, 62.45, 38.27, 21.56; DEPT-135 (75 MHz, DMSO-d_6): one negative peak at δ 38.26 for one 'CH_2' group; COSY (300 MHz, DMSO-d_6): Signal indicating coupling between H of CH_3 (δ 1.64) and H of CH (δ 5.16). The signal indicating coupling between H of CH (δ 5.16) and H of OH (δ 5.82); ESI MS: m/z (M^+) value at 320.04; Anal. Calcd for $C_{18}H_{16}N_4O_2$: C, 67.49; H, 5.03; N, 17.49. Found: C, 67.55; H, 5.14; N, 17.44; Chiral HPLC: Chiralpak IB column of diacel, *i*-PrOH/Hexane 15:85, Flow rate 0.6 mL/min, λ_{max} = 254 nm, t_{major} = 17.69 min, t_{minor} = 12.61, 93% ee.

4.2.2.4. (*S*)-(−)-*N*-(Methyl-1′-benzotriazolyl)-2-(α-hydroxyethyl) benzimidazole Btz-HEB 2d. Compound **2d** was prepared by procedure **B**; colorless solid, 1.77 g, 98% yield; melting point: 135 °C; $[\alpha]_D^{25} = -45$ (*c* 1, $CHCl_3$); IR (KBr, cm^{-1}): ν_{max} 3300, 3094, 1449, 1244, 1011, 745; ^{1}H NMR (300 MHz, DMSO-d_6): δ 8.09–7.74 (m, 4H), 7.66–7.59 (m, 2H), 7.46–7.42 (m, 2H), 7.30–7.20 (m, 2H), 6.03 (d, 1H, J = 6.6 Hz, -OH), 5.39 (t, 1H, J = 6.6 Hz), 1.65 (d, 3H, J = 6.3 Hz.); ^{13}C NMR (75 MHz, DMSO-d_6): δ 156.31, 145.01, 141.58, 134.88, 132.40, 128.48, 128.14, 124.44, 123.03, 122.38, 119.39, 119.35, 110.60, 62.08, 54.50, 21.00; DEPT-135 (75 MHz, DMSO-d_6): one negative peak at δ 54.50 for one 'CH_2' group; COSY (300 MHz, DMSO-d_6): Signal indicating coupling between H of CH_3(δ 1.65)and H of CH(δ 5.39). The signal indicating coupling between H of CH (δ 5.39) and H of OH (δ 6.032); ESI MS: m/z (M^+) value at 293.54; Anal. Calcd for $C_{16}H_{15}N_5O$: C, 65.52; H, 5.15; N, 23.88. Found: C, 65.55; H, 5.08; N, 23.95; Chiral HPLC: Chiralpak IB column of diacel, DCM (20% ethanol)/Hexane 30:70, Flow rate = 0.8 mL/min, λ_{max} = 254 nm, t_{major} = 16.18 min, t_{minor} = 13.30 min, 98% ee.

4.3. Asymmetric Diels–Alder reaction of anthrone 3 and various *N*-substituted maleimides 4a–g

4.3.1. Representative experimental procedure for the Diels–Alder reaction

4.3.1.1. For chiral Tweezer Pyr-HEB 2a. To a 50 mL round bottom flask (RBF) containing Pyr-HEB **2a** (10 mol %) and a stirring bar, anhydrous 1,2-dichloroethane at −10 °C, anthrone **3** (97 mg, 0.5 mmol) and *N*-substituted maleimide **4a–g** (0.5 mmol) were added in this sequence. The reaction was carried out under dry condition and monitored with TLC. After stirring at −10 °C for 8–12 h, on completion, the reaction mixture was acidified with dilute hydrochloric acid and extracted with chloroform. The organic extracts were washed with brine, dried over sodium sulfate and filtered. The solvent was removed in vacuum, purified by using Silica column chromatography (gradient elution with chloroform/pet. ether mixtures; 80:20).

4.3.1.2. For chiral Tweezer Btz-HEB 2d. To a 50 mL RBF containing Btz-HEB **2d** (10 mol %) and a stirring bar, anhydrous Chloroform at room temperature, anthrone **3** (97 mg, 0.5 mmol) and *N*-substituted maleimide **4a–g** (0.5 mmol) were added in this

sequence. The reaction was carried out under dry condition and monitored with TLC. After stirring at room temperature for 12 h, on completion, the reaction mixture was acidified with dilute hydrochloric acid and extracted with chloroform. The organic extracts were washed with brine, dried over sodium sulfate, and filtered. The solvent was removed in vacuum, purified by using silica column chromatography (gradient elution with chloroform/pet. ether mixtures; 80:20).

4.3.1.3. 4-Hydroxy-2-methyl-3a,4,9,9a-tetrahydro-4,9[1′,2′]-benzeno-1*H*-benz[*f*]isoindole-1,3(2*H*)-dione 5a. Colorless solid, 143.4 mg, 94% yield with catalyst **2a**, 129.7 mg, 85% yield with catalyst **2d**; melting point: 184–186 (Lit. 189–190 °C);[4a] ^{1}H NMR (300 MHz, $CDCl_3$): δ 7.69 (m, 1H), 7.48 (m, 1H), 7.36 (m, 1H), 7.34–7.10 (m, 5H), 4.72 (d, 1H, J = 3.3 Hz), 4.42 (s, 1H), 3.32 (dd, 1H, J = 3.6 Hz, J = 8.5 Hz), 3.11 (d, 1H, J = 8.4 Hz), 2.49 (s, 3H); ESI MS: ($C_{19}H_{15}NO_3$) m/z (M^+) value at 304.95; Chiral HPLC: Chiralpak IB column of diacel, *i*-PrOH/Hexane 10:90, Flow rate 0.6 mL/min, λ_{max} = 230 nm, t_{major} = 23.33 min, t_{minor} = 19.64 min, 63% ee; {$[\alpha]_D^{25}$ = +44.1 (c 1, $CHCl_3$)} with catalyst **2a**, 12% ee {$[\alpha]_D^{25}$ = −8.6 (c 1, $CHCl_3$)} with catalyst **2d**.

4.3.1.4. 4-Hydroxy-2-ethyl-3a,4,9,9a-tetrahydro-4,9[1′,2′]-benzeno-1*H*-benz[*f*]isoindole-1,3(2*H*)-dione 5b. Colorless solid, 143.5 mg, 90% yield with catalyst **2a**, 119.6 mg, 75% yield with catalyst **2d**; melting point: 210–212 (Lit. 213–215 °C);[2a] ^{1}H NMR (300 MHz, $CDCl_3$): δ 7.69 (m, 1H), 7.50 (m, 1H), 7.36 (m, 1H), 7.27–7.13 (m, 5H), 4.73 (d, 1H, J = 3.6 Hz), 4.53 (s, 1H), 3.29 (dd, 1H, J = 3.6 Hz, J = 8. Hz), 3.14 (q, 2H), 3.07 (d, 1H, J = 8.7 Hz), 0.40 (t, 3H, J = 7.2 Hz); ESI MS: ($C_{20}H_{17}NO_3$) m/z (M^+) value at 318.96; Chiral HPLC: Chiralpak AD column of diacel, *i*-PrOH/Hexane 10:90, Flow rate 0.6 mL/min, λ_{max} = 230 nm, t_{major} = 26.97 min, t_{minor} = 24.27 min, 88% ee; {$[\alpha]_D^{25}$ = +33.7 (c 1, $CHCl_3$)} with catalyst **2a**, 23% ee; {$[\alpha]_D^{25}$ = −9.1 (c 1, $CHCl_3$)} with catalyst **2d**.

4.3.1.5. 4-Hydroxy-2-propyl-3a,4,9,9a-tetrahydro-4,9[1′,2′]-benzeno-1*H*-benz[*f*]isoindole-1,3(2*H*)-dione 5c. Colorless solid, 149.8 mg, 90% yield with catalyst **2a**, 146.5 mg, 88% yield with catalyst **2d**; melting point: 218–220 °C; ^{1}H NMR (300 MHz, CDCl3): δ 7.69 (m, 1H), 7.50 (m, 1H), 7.34 (m, 1H), 7.27–7.13 (m, 5H), 4.72 (d, 1H, J = 3.6 Hz), 4.52 (s, 1H), 3.29 (dd, 1H, J = 3.6 Hz, J = 8.5 Hz), 3.08 (q, 2H), 3.01 (d, 1H), 0.79 (m, 2H), 0.54 (t, 3H, J = 7.5 Hz); ESI MS: ($C_{21}H_{19}NO_3$); m/z (M^+) value at 333.02; Chiral HPLC: Chiralpak IB column of diacel, *i*-PrOH/Hexane 10:90, Flow rate 0.6 mL/min, λ_{max} = 230 nm, t_{major} = 19.87 min, t_{minor} = 15.55 min, 14% ee; {$[\alpha]_D^{25}$ = +5.7 (c 1, $CHCl_3$)} with catalyst **2a**, 22% ee; {$[\alpha]_D^{25}$ = −8.5 (c 1, $CHCl_3$)} with catalyst **2d**.

4.3.1.6. 4-Hydroxy-2-*t*-butyl-3a,4,9,9a-tetrahydro-4,9[1′,2′]-benzeno-1*H*-benz[*f*]isoindole-1,3(2H)-dione 5d. Colorless solid, 150.9 mg, 87% yield with catalyst **2a**, 137 mg, 79% yield with catalyst **2d**; melting point: 212–215 (Lit. 217–219 °C);[2c] ^{1}H NMR (300 MHz, $CDCl_3$): δ 8.35 (m, 1H), 7.87 (m, 1H), 7.37 (dd, 1H), 7.27–7.17 (m, 5H), 4.72 (s, 1H), 4.69 (d, J = 3.6 Hz, 1H), 3.17 (dd, 1H, J = 3.6 Hz, J = 9.0 Hz), 2.95 (d, 1H, J = 9.0 Hz), 1.14 (s, 9H); ESI MS: ($C_{22}H_{21}NO_3$) m/z (M^+) value at 346.76. Chiral HPLC: Chiralpak IB column of diacel, *i*-PrOH/Hexane 10:90, Flow rate 0.6 mL/min, λ_{max} = 230 nm, t_{major} = 16.27 min, t_{minor} = 10.79 min, 48% ee; {$[\alpha]_D^{25}$ = +12 (c 1, $CHCl_3$)} with catalyst **2a**, 30% ee {$[\alpha]_D^{25}$ = −8.2 (c 1, $CHCl_3$)} with catalyst **2d**.

4.3.1.7. 4-Hydroxy-2-benzyl-3a,4,9,9a-tetrahydro-4,9[1′,2′]-benzeno-1*H*-benz[*f*]isoindole-1,3(2*H*)-dione 5e. Colorless solid, 142.8 mg, 75% yield with catalyst **2a**, 163.7 mg, 86% yield with catalyst **2d**; melting point: 207–209 (Lit. 211–213 °C);[4a] ^{1}H NMR (300 MHz, $CDCl_3$): δ 7.58 (m, 1H), 7.49 (m, 1H), 7.40 (m, 1H), 7.21–7.03 (m, 8H), 6.32 (m, 2H), 4.71 (d, 1H, J = 3.3 Hz), 4.56 (s, 1H), 4.25 (s, 2H), 3.40 (dd, 1H, J = 3.3 Hz, J = 8.1 Hz), 3.23 (d, 1H, J = 8.7 Hz); ESI MS: ($C_{25}H_{19}NO_3$) m/z (M^+) value at 380.86. Chiral HPLC: Chiralpak IB column of diacel, *i*-PrOH/Hexane 20:80, Flow rate 0.6 mL/min, λ_{max} = 230 nm, t_{major} = 21.16 min, t_{minor} = 25.72 min, 78% ee; {$[\alpha]_D^{25}$ = +36.5 (c 1, $CHCl_3$)} with catalyst **2a**, 24% ee {$[\alpha]_D^{25}$ = −13.6 (c 1, $CHCl_3$)} with catalyst **2d**.

4.3.1.8. 4-Hydroxy-2-phenyl-3a,4,9,9a-tetrahydro-4,9[1′,2′]-benzeno-1*H*-benz[*f*]isoindole-1,3(2*H*)-dione 5f. Colorless solid, 119.3 mg, 65% yield with catalyst **2a**, 167 mg, 91% yield with catalyst **2d**; melting point: 204–205 (Lit. 208–209 °C);[4a] ^{1}H NMR (300 MHz, $CDCl_3$): δ 7.73 (d, 1H, J = 7.2 Hz), 7.56 (d, 1H, J = 7.2 Hz),7.41 (d, 1H, J = 6.9 Hz),7.36–7.21 (m, 8H), 6.51–6.47 (m, 2H), 4.84 (d, 1H, J = 3.3 Hz), 4.57 (s, 1H, OH),3.47 (dd, 1H, J = 3.6 Hz, J = 8.7 Hz), 3.26 (d, 1H, J = 8.7 Hz); ESI MS: ($C_{24}H_{17}NO_3$) m/z (M^+) value at 366.80. Chiral HPLC: Chiralpak IB column of diacel, *i*-PrOH/Hexane 20:80, Flow rate 0.6 mL/min, λ_{max} = 230 nm, t_{major} = 27.24 min, t_{minor} = 34.56 min, 17% ee; {$[\alpha]_D^{25}$ = +9.8 (c 1, $CHCl_3$)} with catalyst **2a**, 73% ee {$[\alpha]_D^{25}$ = −38.7 (c 1, $CHCl_3$)} with catalyst **2d**.

4.3.1.9. 4-Hydroxy-2-(4-methoxyphenyl)-3a,4,9,9a-tetrahydro-4,9[1′,2′]-benzeno-1*H*-benz[*f*]isoindole-1,3(2*H*)-dione 5g. Colorless solid, 119.1 mg, 60% yield with catalyst **2a**, 162.7 mg, 82% yield with catalyst **2d**; melting point: 203–205 (Lit. 206–207 °C);[4a] ^{1}H NMR (300 MHz, $CDCl_3$): δ 7.40 (m, 3H), 7.33–7.23 (m, 5H), 6.79 (d, 2H, J = 9.0 Hz), 6.37 (d, 2H, J = 8.7 Hz), 4.83 (d, 1H, J = 3.6 Hz), 4.50 (s, 1H, OH), 3.76 (s, 3H), 3.45 (dd, 1H, J = 3.6 Hz, J = 8.7 Hz),3.24 (d, 1H, J = 8.7 Hz); ESI MS: ($C_{25}H_{19}NO_4$) m/z (M^+) value at 396.81. Chiral HPLC: Chiralpak IB column of diacel, *i*-PrOH/Hexane 20:80, Flow rate 0.6 mL/min, λ_{max} = 230 nm, t_{major} = 29.15 min, t_{minor} = 31.57 min, 16% ee; {$[\alpha]_D^{25}$ = +4.2 (c 1, $CHCl_3$)} with catalyst **2a**, 23% ee; {$[\alpha]_D^{25}$ = −5.7 (c 1, $CHCl_3$)} with catalyst **2d**.

Acknowledgment

Authors are thankful to UGC-BSR, India, for financial support.

Supplementary data

Supplementary data associated with this article can be found, in the online version, at http://dx.doi.org/10.1016/j.tetasy.2016.01.002.

References

1. (a) Ishihara, J.; Nakadachi, S.; Watanabe, Y.; Hatakeyama, S. *J. Org. Chem.* **2015**, *80*, 2037–2041; (b) Carmona, D.; Lamata, M. P.; Pardo, P.; Rodrıguez, R.; Lahoz, F. J.; Orduna, P. G.; Alkorta, I.; Elguero, J.; Oro, L. A. *Organometallics* **2014**, *33*, 616–619; (c) Sakaguchi, Y.; Iwade, Y.; Sekikawa, T.; Minami, T.; Hatanaka, Y. *Chem. Commun.* **2013**, 11173–11175.
2. (a) Mirgane, N. A.; Karnik, A. V. *Chirality* **2011**, *23*, 404–407; (b) Hau, C. K.; He, H.; Lee, A. W. M.; Chik, D. T. W.; Cai, Z.; Wong, H. N. C. *Tetrahedron* **2010**, *66*, 9860–9874; (c) Akalay, D. G.; Durner, J. W.; Bats, D.; Gobel, M. W. *Beilstein J. Org. Chem.* **2008**, *4*, 28; (d) Zea, A.; Valerao, G.; Alba, A.; Moyano, A.; Rios, R. *Adv. Synth. Catal.* **2010**, *352*, 1102–1106; (e) Zea, A.; Alba, A.; Bravo, N.; Moyano, A.; Rios, R. *Tetrahedron* **2011**, *67*, 2513–2529; (f) Kumagai, J.; Otsuki, T.; Reddy, U. V.; Kohari, Y.; Seki, C.; Uwai, K.; Okuyama, Y.; Kwon, E.; Tokiwa, M.; Takeshita, M.; Nakano, H. *Tetrahedron: Asymmetry* **2015**, *26*, 1423–1429.
3. (a) Riant, O.; Kagan, H. B. *Tetrahedron* **1994**, *50*, 4543–4554; (b) Riant, O.; Kagan, H. B. *Tetrahedron Lett.* **1989**, *30*, 7403–7406.
4. (a) Uemae, K.; Masuda, S.; Yamamoto, Y. *J. Chem. Soc., Perkin Trans. 1* **2001**, 1002–1006; (b) Tokioka, K.; Masuda, S.; Fijii, T.; Hata, Y.; Yamamoto, Y. *Tetrahedron: Asymmetry* **1997**, *8*, 101–107.
5. (a) Sun, W.; Zhu, G.; Wu, C.; Li, G.; Hong, L.; Wang, R. *Angew. Chem., Int. Ed.* **2013**, *52*, 8633–8637; (b) Anderson, J. C.; Koovits, P. *J. Chem. Sci.* **2013**, *4*, 2897–2901; (c) Bera, K.; Namboothiri, I. N. N. *J. Org. Chem.* **2015**, *80*, 1402–1413; (d) Bera, K.; Namboothiri, I. N. N. *Org. Lett.* **2012**, *14*, 980–983.

6. (a) Momiyama, N.; Torii, H.; Saito, S.; Yamamoto, H. *PNAS* **2004**, *101*, 5374–5378; (b) Tang, Z.; Cun, L. F.; Cui, X.; Mi, A. Q.; Jiang, Y. Z.; Gong, L. Z. *Org. Lett.* **2006**, *8*, 1263–1266.
7. (a) Shen, J.; Nguyen, T. T.; Goh, Y. P.; Ye, W.; Fu, X.; Xu, J.; Tan, C. H. *J. Am. Chem. Soc.* **2006**, *128*, 13692–13693; (b) Zou, L.; Wang, B.; Mu, H.; Zhang, H.; Song, Y.; Qu, J. *Org. Lett.* **2013**, *15*, 3106–3109; (c) Fang, B.; Liu, X.; Zhao, J.; Tang, Y.; Lin, L.; Feng, X. *J. Org. Chem.* **2015**, *80*, 3332–3338.
8. (a) Torres, E. G.; Alonso, D. A.; Bengoa, E. G.; Najera, C. *Eur. J. Org. Chem.* **2013**, 1434–1440; (b) Xu, D. Q.; Wang, L. P.; Luo, S. P.; Wang, Y. F.; Zhang, S.; Xu, Z. Y. *Eur. J. Org. Chem.* **2008**, 1049–1053; (c) Cobb, A. J. A.; Longbottom, D. A.; Shaw, D. M.; Ley, S. V. *Chem. Commun.* **2004**, 1808–1809.
9. (a) Lu, H.; Bai, J.; Xu, J.; Yang, T.; Lin, X.; Li, J.; Ren, F. *Tetrahedron* **2015**, *71*, 2610–2615; (b) Milla, P. V.; Sansano, J. M.; Nájera, C.; Fiser, B.; Bengoa, E. G. *Eur. J. Org. Chem.* **2015**, 2614–2621.
10. Bai, J. F.; Guo, Y. L.; Peng, L.; Jia, L. N.; Xu, X. Y.; Wang, L. X. *Tetrahedron* **2013**, *69*, 1229–1233.
11. (a) Sun, X.; Worthy, A. D.; Tan, K. L. *J. Org. Chem.* **2013**, *78*, 10494–10499; (b) Sheppard, C. I.; Taylor, J. L.; Wiskur, S. L. *Org. Lett.* **2011**, *13*, 3794–3797.
12. (a) Blackmond, D. G.; Moran, A.; Hughes, M.; Armstrong, A. *J. Am. Chem. Soc.* **2010**, *132*, 7598–7599; (b) Cai, F. Y.; Li, L.; Luo, M. X.; Yang, K. F.; Lai, G. Q.; Jiang, J. X.; Xu, L. W. *Chirality* **2011**, *23*, 397–403; (c) Bartok, M. *Chem. Rev.* **2010**, *110*, 1663–1705.
13. Ikariya, T.; Ishii, Y.; Kawano, H.; Arai, T.; Saburi, M.; Yoshikawa, S.; Akutagawa, S. *J. Chem. Soc., Chem. Commun.* **1985**, 922–924.
14. (a) Szollosi, G.; Bartok, M. *Chirality* **2001**, *13*, 614–618; (b) London, G.; Szollosi, G.; Bartok, M. *J. Mol. Catal. A: Chem.* **2007**, *267*, 98–101.
15. Fenninger, A. P. *Synthesis* **1986**, *2*, 89–116.
16. Kuwano, R.; Sawamura, M.; Ito, Y. *Bull. Chem. Soc. Jpn.* **2000**, *73*, 2571.
17. (a) Trost, B. M.; Fettes, A.; Shireman, B. T. *J. Am. Chem. Soc.* **2004**, *126*, 2660–2661; (b) Casey, C. P.; Martins, S. C.; Fagan, M. A. *J. Am. Chem. Soc.* **2004**, *126*, 5585–5592; (c) Sibi, M. P.; Gorikunti, U.; Liu, M. *Tetrahedron* **2002**, *58*, 8357–8363.
18. Zhou, J.; Ye, M. C.; Huang, Z. Z.; Tang, Y. *J. Org. Chem.* **2004**, *69*, 1309–1320.
19. (a) Kobayashi, S.; Ishitani, H. *J. Am. Chem. Soc.* **1994**, *116*, 4083–4084; (b) Furegati, M.; Rippert, A. J. *Tetrahedron: Asymmetry* **2005**, *16*, 3947–3950.
20. (a) Du, D. M.; Lu, S. F.; Fang, T.; Xu, J. *J. Org. Chem.* **2005**, *70*, 3712–3715; (b) Lu, S. F.; Du, D. M.; Zhang, S. W.; Xu, J. *Tetrahedron: Asymmetry* **2004**, *15*, 3433–3441.
21. (a) Zaitsev, A. B.; Adolfsson, H. *Org. Lett.* **2006**, *8*, 5129–5132; (b) Kobayashi, S.; Horibe, M. *J. Am. Chem. Soc.* **1994**, *116*, 9805–9806.